OPEN-MIDPLANE GRADIENT PERMANENT MAGNET WITH 1.53 T PEAK FIELD*

S.J. Brooks†, Brookhaven National Laboratory, Upton, NY, USA

Abstract

The CEBAF energy upgrade [1] will require magnets with high fields to bend electron beams of up to 22 GeV in the 80.6 m radius tunnel. A peak field in excess of 1.5 T, together with a large gradient of 40 T/m or more, are used in its fixed-field arc lattice to bend multiple recirculation energies in a single pipe. Additionally, the magnet must have an open midplane to allow synchrotron radiation to be absorbed by a cooling channel.

A short 45 mm section of NdFeB prototype has been designed and built as part of permanent magnet R&D at BNL. This satisfies all the above requirements and has had its integrated field tuned to better than 1 part in 10^3. This tuning process uses a technique with iron rods [2] adapted from CBETA [3, 4] and miniaturised here, together with measurements at a new compact field-mapping stand that is accurate to 1 part in 10^4.

SPECIFICATION

The requirements for the prototype permanent magnet are given in Table 1. The combined-function field, gradient and good field region were taken from the lattice of the fixed-field (FFA) arcs for the CEBAF energy upgrade [1]. This is evolving and has changed since last reported [5] and continued to change after the prototype magnet was ordered. As of early 2023, only one FFA loop is required in the upgrade, consisting of two slightly different 180° arcs each with two distinct types of permanent magnet. The parameter ranges required in this most up-to-date lattice as of writing are: dipole $-1.2815 \le B(0) \le -0.3828$ T, gradient $41.13 \le |B'| \le 53.79$ T/m and $1.515 \le B_{\max} \le 1.573$ T, which are still well represented by the prototype. Designs of similar geometry exist for all four magnets in the new lattice.

The prototype magnet was built as a small 45 mm length section in order to test the integrated field per unit length. In reality, many sections will be clamped together longitudinally to make the full magnet, which will be roughly 1–2 m long. Initially, 60 mm sections were asked for but there was a Neodymium ore price spike in early 2022, together with pandemic-related supply chain issues, making the material particularly expensive to obtain at that point.

The vertical full aperture of 15 mm is about the minimum required to fit a beam pipe and any iron field tuning rods, while still having space for beam.

Neodymium Iron Boron (NdFeB) material was selected to give the high fields required to bend the beam in the fixed radius CEBAF tunnel, while also selecting the high-coercivity (high temperature) grade N42EH [6], which sacrifices some of this field strength for improved radiation resistance and general resistance to demagnetisation: it can withstand 2.9 T of reverse field before losing all its magnetisation.

Table 1: Prototype Magnet Specification

Parameter	Value	Unit
Dipole ($B(0)$)	−0.9512	T
Gradient (B')	55.54	T/m
x good field region (GFR)	±10.5	mm
$B_{\max}$ in GFR	(−)1.536	T
Magnet length	45	mm
Vertical aperture (GFR)	±7.5	mm
Minimum midplane gap	±3	mm
Material	NdFeB	
Grade	N42EH	
B_r	1.28–1.33	T
$\mu_0 H_{cJ}$	2.9	T

DESIGN AND FEATURES

The cross-section of the magnet is shown in Fig. 1 and has area 70.1 cm^2. It consists of 24 wedge-shaped pieces of NdFeB with geometry given in Table 2. The outer wedges are symmetrical, while the top and bottom wedges have two edges parallel to the horizontal axis. The wedge shape prevents the pieces from falling into the aperture under magnetic forces, although some of the wedges here are quite narrow, so future magnets will bind them in place with epoxy.

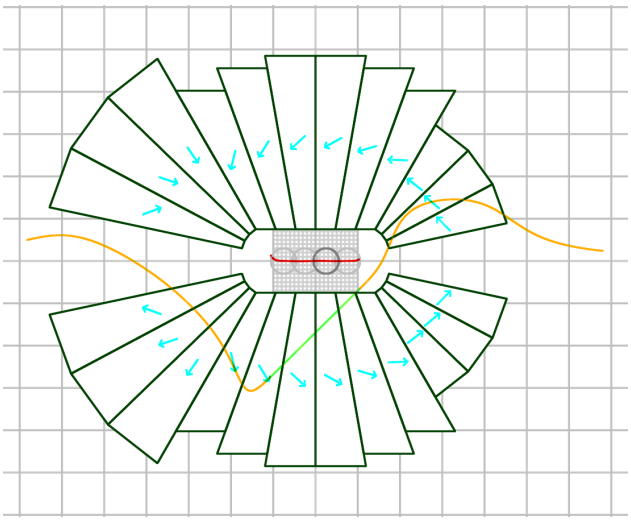

Figure 1: 2D permanent magnet design (cm grid). Midplane field is graphed in orange, with good field region in green.

* Work supported by Brookhaven Science Associates, LLC under Contract No. DE-SC0012704 with the U.S. Department of Energy.

† sbrooks@bnl.gov

Table 2: Permanent Magnet Geometry

Parameter	Value
Number of wedges	24 (3+6+3 per side)
Midplane anglular gap	±12°
Wedge opening angles	16°/10°/16°

Each wedge has a different magnetisation direction, although when comparing the magnetisation vectors of symmetrical upper and lower blocks, the horizontal component is inverted while the vertical stays the same. The field on the midplane good field region, calculated by a 2D simulation, differs by no more than 6.8 Gauss, or 4.4×10^{-4} of the peak field, from the ideal value.

The orientation of the magnetisation in each wedge, as well as the wedge height, were determined by multi-parameter optimisation similar to that used in the author's HalbachArea tool [7]. The figure of merit was RMS field error in the midplane good field region.

The magnet has an open midplane to let synchrotron radiation emitted by the horizontally-bent high-energy electrons escape, but unlike the designs in [5], the midplane gap now has an opening angle. This helps greatly with the mechanical strength of the vacuum chamber, as only a small distance of the unsupported span has to be of minimum thickness, with the material thickening as the midplane gap grows.

The central beam aperture is oval rather than circular, as this significantly reduces the amount of permanent magnet material required for a given horizontal orbit excursion [8].

Field Tuning Method

Given an initial measurement of the magnet's field, small iron rods can be placed just inside the aperture to cancel field errors, following the method in [2]. This was adapted for a smaller aperture magnet by using rods of 0.89 mm (35 mil) diameter, reduced from 2.03 mm (80 mil), and adapted for the oval aperture by placing the rods above and below the midplane, as shown in Fig. 2. The aperture appears tilted as the software also fits for magnet orientation on the measurement stand. It was found that 26 rods placed at $y = \pm 6.66$ mm and spaced by $\Delta x = 2.25$ mm out to $|x|_{\max} = 13.5$ mm were sufficient to give good error correction in simulations.

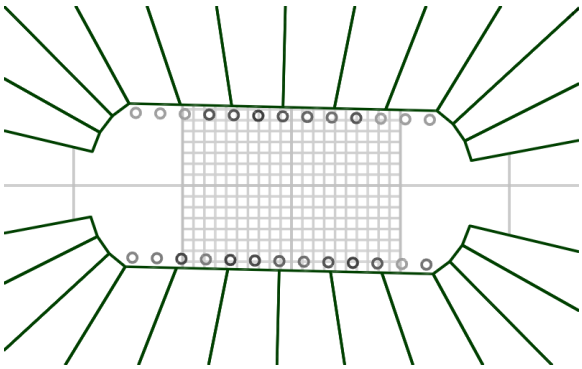

Figure 2: Locations of field tuning rods within the aperture.

CONSTRUCTION

This prototype magnet was made by placing the NdFeB wedges within a 3D printed PLA mould, contained by a rectangular aluminium frame, as shown in Figures 3 and 4.

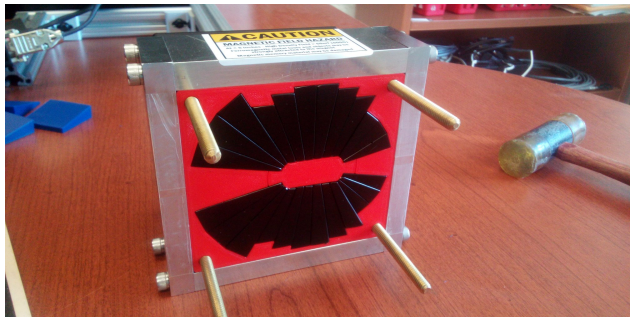

Figure 3: Magnet before central plastic plug is removed.

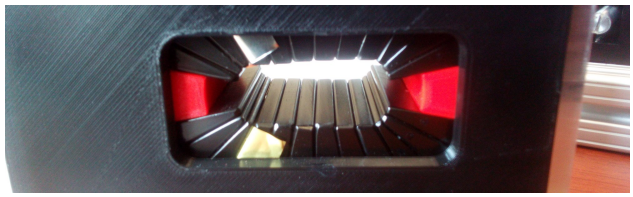

Figure 4: Aperture of magnet after central plug removed.

The forces and torques between permanent magnet wedges are too large for assembly purely by hand, so channels to guide the magnets were 3D printed and attached to the mould, as shown in Fig. 5. The mould was initially filled with plastic dummy wedges, which were replaced one-at-a-time by magnets. This was done by sliding the magnet down the channel and pushing out the dummy wedge, which also serves as the longitudinal end-stop.

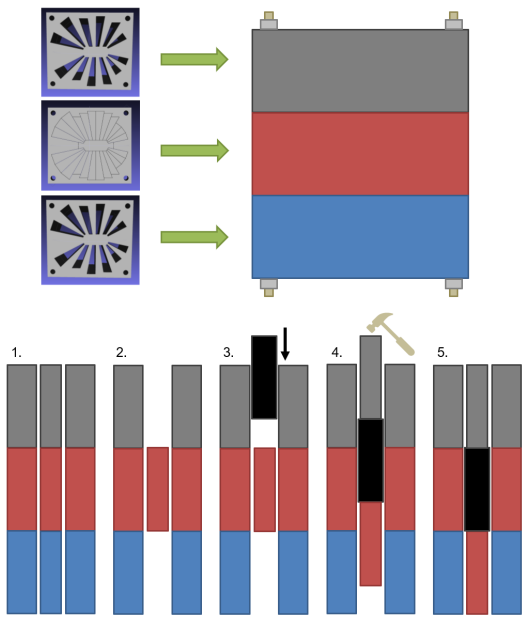

Figure 5: Assembly tooling and magnet insertion process.

Field Tuning Rod Holders

Plastic holders with channels to align the iron tuning rods within the magnet were 3D printed, as shown in Fig. 6.

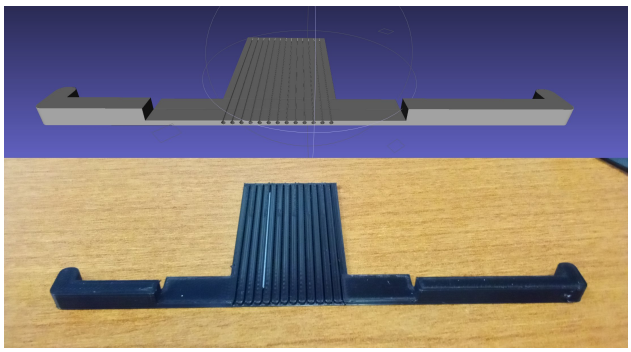

Figure 6: Tuning rod holder design and 3D printed part.

FIELD MEASUREMENTS

Field mapping was done using a Senis 3MH6 Teslameter with a three-axis Hall probe that has ±0.01% accuracy. Two stacked linear stages, seen in Fig. 7, scanned transversely and longitudinally in the magnet. The accuracy of these stages was determined to be 1–2 μm by cross-checking against the magnet field when the same point was approached from different directions. All of this leads to a capability of measuring the magnetic field at the 10^{-4} level.

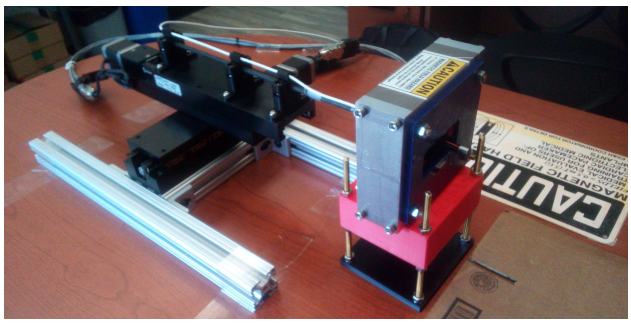

Figure 7: Field mapping the magnet midplane with a three-axis Hall probe moving transversely and longitudinally.

The linear stages have a full range of 200 mm but in this case $x = \pm 12$ mm was scanned transversely in 0.5 mm steps and the full range was scanned longitudinally in 2.5 mm steps to give the integrated field.

Table 3: Measured integrated magnetic field errors in the good field region, in units of 10^{-4} of the maximum field.

Tuning iteration	B_y **max error**	B_x **max error**	**B vector RMS error**
Original	41.44	12.36	27.44
1	21.03	7.06	17.30
2	11.22	3.41	9.20
3	7.88	6.56	5.62

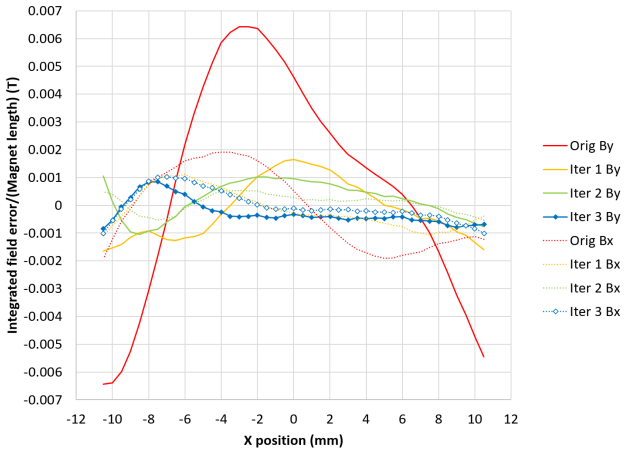

Figure 8: Integrated field error as a function of transverse position in the magnet, for successive field tuning iterations.

Integrated field measurements of the magnet and three successive field tuning iterations are shown in Fig. 8 and Table 3. These are given as deviations from the ideal linear integrated field, as otherwise the differences would be too small to see on a plot. They are also presented as a function of transverse position, since multipole harmonics on a circle are no longer easy to define for an oval aperture magnet. Only the $x = \pm 10.5$ mm good field region is shown in Fig. 8 and used for error statistics.

The field improves to better than 1 part in 10^3 in both B_y and B_x error components. This is roughly the field quality criterion used for accepting the CBETA magnets [2]. It is likely that three tuning iterations are needed because of how short this R&D magnet is, as the longer magnets from CBETA typically converged in one or two iterations. Field contributions from the tuning rods in a short magnet will be less well-approximated by the 2D model.

The main source of the original magnet's large B_y error contribution (4.1×10^{-3} relative) could be wedges 'falling' in to different heights around the aperture under magnetic forces, as can be seen by looking closely at Fig. 4. Top-bottom symmetric effects, such as this, produce B_y errors, whereas B_x (skew) errors come from asymmetric effects, which were smaller here.

CONCLUSION

The prototype permanent magnet demonstrates:

- High combined-function field levels up to 1.536 T;
- Zero energy consumption;
- Good linearity with relative errors $< 10^{-3}$;
- An open midplane for synchrotron radiation emission, with opening angle for a stronger vacuum chamber;
- An oval aperture for lower material use and cost.

These features are key for the 20 GeV CEBAF energy upgrade [1], as well as advanced light source lattices that use high-gradient magnets [9] and compact fixed-field hadron therapy gantries using permanent magnets [10].

REFERENCES

[1] R. M. Bodenstein *et al.*, "Current Status of the FFA@CEBAF Energy Upgrade Study", presented at the 13th Int. Particle Accelerator Conf. (IPAC'22), Bangkok, Thailand, June 2022, paper THPOST023, pp.2494–2496.

[2] S. Brooks, G. Mahler, J. Cintorino, J. Tuozzolo, and R. Michnoff, "Permanent magnets for the return loop of the Cornell-Brookhaven energy recovery linac test accelerator", *Phys. Rev. Accel. Beams*, vol. 23, p. 112401, Nov 2020. doi:10.1103/PhysRevAccelBeams.23.112401

[3] A. Bartnik *et al.*, "CBETA: First Multipass Superconducting Linear Accelerator with Energy Recovery", *Phys. Rev. Lett.*, vol. 125, p. 044803, 2020. doi:10.1103/PhysRevLett.125.044803

[4] G. H. Hoffstaetter *et al.*, "CBETA Design Report, Cornell-BNL ERL Test Accelerator", 2017. arXiv:1706.04245

[5] S. J. Brooks, and S. A. Bogacz, "Permanent Magnets for the CEBAF 24 GeV Upgrade", presented at the 13th Int. Particle Accelerator Conf. (IPAC'22), Bangkok, Thailand, June 2022, paper THPOTK011, pp.2792–2795.

[6] Allstar Magnetics neodymium permanent magnet specifications, https://allstarmagnetics.com/permanent-magnets/#neo

[7] HalbachArea tool, https://stephenbrooks.org/ap/halbacharea/

[8] S. J. Brooks, "Modified Halbach Magnets for Emerging Accelerator Applications", presented at the 12th Int. Particle Accelerator Conf. (IPAC'21), Campinas, Brazil, May 2021, paper TUXC07, pp.1315–1318.

[9] G. Wang, T. Shaftan *et al.*, "Complex bend. II. A new optics solution", *Phys. Rev. Accel. Beams*, vol. 22, p. 110703, 2019. doi:10.1103/PhysRevAccelBeams.22.110703

[10] D. Trbojevic, S. J. Brooks, T. Roser, and N. Tsoupas, "Superb Fixed Field Permanent Magnet Proton Therapy Gantry", presented at the 12th Int. Particle Accelerator Conf. (IPAC'21), Campinas, Brazil, May 2021, paper TUPAB030, pp.1405–1408.